

## Formation of Calcium Phosphate Minerals in the Presence of Fetuin-A

Şeniz Uçar<sup>1\*</sup> 

<sup>1</sup> Department of Chemical Engineering, Norwegian University of Science and Technology, Trondheim, Norway

\*[seniz.ucar@ntnu.no](mailto:seniz.ucar@ntnu.no)

\*Orcid: 0000-0002-5549-6061

Received: 17 December 2021

Accepted: 15 August 2022

DOI: 10.18466/cbayarfbe.1038019

### Abstract

Mineral formation is regulated by molecular based promoters or inhibitors in biological systems. Among serum proteins, fetuin-A can effectively inhibit unwanted calcification *in vivo* via forming fetuin-mineral complexes called calciprotein particles (CPPs). Here, the formation and phase transformation mechanisms of CPPs are investigated in detail by combining *in situ* potentiometric measurements and solid phase characterization. It is found that fetuin-A inhibits mineral formation via affecting both thermodynamic and kinetic factors of precipitation. A better understanding of the reaction pathway as well as the interactions between the mineral and protein counterparts can potentially inform the development of *in vitro* model systems of biomineralization and pave the way for the development of new therapies to treat ectopic calcification.

**Keywords:** Biomineralization, calcium phosphate, fetuin-A, mineral formation

### 1. Introduction

Mineral formation *in vivo* is a complex process that involves organic phases, which regulate the nucleation, growth, morphology and organization of biogenic minerals that form the major solid inorganic component of hard tissues in many different organisms [1]. This intricate and well-regulated process results in composite materials with exceptional features that are exploited by the organisms for a variety of purposes and through active control mechanisms on mineral formation, their biophysical properties are optimized for specific functions. The key control mechanisms that involve the regulation of chemistry, structure and morphology to direct the skeletal biomineralization processes also play significant roles in the prevention of pathological calcification [2]. The blood serum in humans is supersaturated with respect to multiple calcium phosphate (CaP) phases, meaning that mineral deposition is possible in all compartments with extracellular fluid [3]. However, ectopic mineralization is regulated in body via a variety of control mechanisms and failure to prevent extraosseous calcification is commonly observed with chronic kidney and inflammatory diseases, or aging [4].

Control of mineral nucleation and growth by utilizing molecular based promoters or inhibitors is a common strategy in biological systems [5]. Among serum

proteins, fetuin-A is shown to be one of the most efficient inhibitors of unwanted calcification [6]. Fetuin-A, also known as  $\alpha_2$ -Heremans Schmidt glycoprotein in humans, is an acidic glycoprotein circulating in the serum at a concentration range of 0.3-1.0 mg mL<sup>-1</sup> in healthy individuals [7]. It shows high affinity to calcium ions via the aspartic and glutamic acid rich residues that are mostly negatively charged at physiological conditions [8]. Moreover, the distance between these residues are compatible with the lattice constant of basic calcium phosphates such as octacalcium phosphate and apatite, which explains the high affinity of fetuin-A to bone minerals [9]. The significance of fetuin-A as a mineralization inhibitor has been well documented with both *in vitro* and *in vivo* studies [10, 11]. It is hypothesized that via formation and stabilization of a fetuin-mineral complex (also called calciprotein particles, CPPs), the spontaneous precipitation of calcium phosphate minerals is inhibited in the serum [12]. Previous studies investigating the formation of these complexes suggested that the initial CPPs, CPP-1, are composed of fetuin-A coated amorphous calcium phosphate (ACP) particles, where the lifetime of the highly transient amorphous phase is prolonged by surface stabilization with the protein [13, 14]. Overtime, CPP-1 develops crystallinity and transforms into the secondary CPP, CPP-2, that constitutes an octacalcium phosphate (OCP) or hydroxyapatite (HA) core [15]. Extensive work on the fetuin-CaP system agrees on the

2-step mechanism and has unraveled the features of these mineral-protein complexes [4]. However, the precise function of fetuin-A during the initial stage of the fetuin-mineral complex formation and phase transformation remain obscure. This is mainly due to the poorly understood mechanism of ACP formation even without the additives, and investigation of fetuin-CaP systems in complex biological media where it is difficult to decouple the interactions between fetuin and mineral phase. Therefore, this work pursues to gain more insight on the modes of interaction between the organic and inorganic phases that form CPPs at different stages of mineralization and generate a comprehensive understanding of the interactions between fetuin-A and CaP minerals.

In this work, detailed investigations of solution chemistry are employed via *in situ* monitoring of the reaction media and coupled with characterization of the solid phase. A better understanding of the reaction pathway as well as the interactions between the mineral and protein counterparts can potentially inform the development of *in vitro* model systems of biomineralization and pave the way for the development of new therapies to treat ectopic calcification.

## 2. Materials and Methods

### 2.1. Materials

All chemical reagents were purchased from Sigma-Aldrich. Lyophilized bovine fetuin-A (Sigma F3385) was used as received. Ultrapure deionized water (resistivity 18.2 MΩ cm at 25°C) was used to prepare all aqueous solutions.

### 2.2. Methods

All experiments were carried out in a magnetically stirred 0.5 L double-walled glass reactor. Two baffles were attached to the lid to ensure homogeneous mixing in the reaction medium. Temperature was controlled by a water bath at 25°C for all experiments. This temperature was chosen to minimize the fluctuations during product collection via filtration. In order to prevent intrusion of atmospheric carbon dioxide, nitrogen gas, saturated with water, was constantly bubbled into solutions 2 h prior to and during the experiments. The chemical speciation and activity-based supersaturation,  $S$ , were determined by the thermodynamic calculation programs PHREEQC Interactive 3.1 (U.S. Geological Survey, Reston, VA, USA) and Visual Minteq 3.0 (KTH, Royal Institute of Technology, Stockholm, Sweden), using the Minteq v4 database. All equilibrium constants used for calculations of solution speciation are provided in the supplementary information (supplementary information, section A and Table S1). Supersaturation with respect to different calcium phosphate phases were calculated according to Equation 1, where the multiplication of the activities of

precursor ions are divided by the solubility product,  $K_{sp}$ , for a given phase.

$$S_{CaP} = \left( \frac{a_{Ca}^x \cdot a_{PO_4}^y \cdot a_{OH}^z}{K_{sp,CaP}} \right)^{\frac{1}{x+y+z}} \quad (\text{Eq.1})$$

The pH was measured with 2 s intervals via a combined glass electrode and calcium ion activity was monitored online via a calcium ion specific electrode. Both measurements were continuously recorded with Tiamo software (Metrohm AG, Herisau, Switzerland). Both electrodes were calibrated daily (supplementary information, section B). Spontaneous precipitation of calcium phosphate was induced in semi-batch experiments by allowing precipitation to occur from supersaturated solutions ( $S_{HA} = 25.6$ ) under constant stirring (300 rpm), as described elsewhere [16]. Briefly, 2.4 mM  $KH_2PO_4$  solution containing 50 mM  $KNO_3$  for ionic strength adjustment and KOH to adjust the final pH to  $7.40 \pm 0.02$ , was prepared in a total volume of 250 mL. 50 mM and 20 mL  $Ca(NO_3)_2 \cdot 4H_2O$  solution was then added in the reaction medium at a rate of 0.4 mL  $min^{-1}$  via an automated dosing unit (907 Titrand, Metrohm AG, Herisau, Switzerland).

The concentrations of the precursor solutions were set to evoke a multistep precipitation pathway within a reasonable experimental time and with sufficient product. In experiments with fetuin-A, the corresponding amount of protein solution that will give a total of 5 or 10 mg of fetuin-A in the reaction medium, was added in the phosphate solution. Fresh solutions were prepared for each experiment and filtered through 0.22 μm sterile vacuum filtration systems prior to experiments. Minimum 2 parallel experiments were conducted for each experimental condition.

Solid phases collected at different stages of the reactions were characterized via powder X-ray Diffraction (XRD) (D8 Advance, Bruker AXS GmbH) in the 2θ range of 4-75° with a step size of 0.013° and a step time of 0.67 s. Fourier transform infrared (FTIR) (Tensor, Bruker AXS GmbH) spectra of powder samples were collected between 4000-550  $cm^{-1}$  by averaging 75 scans. Scanning electron microscopy (SEM) (Apreo, FEI) was performed at an accelerating voltage of 2-5 kV. Prior to imaging samples were coated with gold.

## 3. Results and Discussion

### 3.1. Two-step precipitation pathway

Calcium phosphate (CaP) mineralization was achieved by establishing supersaturation in the reaction medium via slow titration of calcium solution, and allowing the spontaneous precipitation to occur. During the course of the reaction, solution pH was continuously monitored and succeeding steps of the reaction were identified via the distinct drops in the monitored signal (Figure 1).

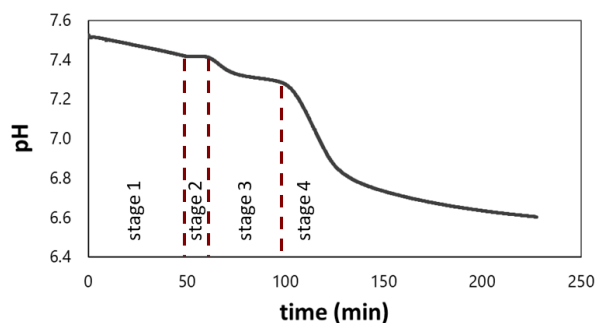


**Figure 1.** pH of the solution during the precipitation reaction in time, and the succeeding stages of the reaction determined by the distinct changes in the signal profile.

Experiments were initiated by slow titration of 20 mL calcium solution into the reaction medium that contained the phosphate solution. This duration is marked as stage 1, and lasts for 50 min. A linear decrease in solution pH was observed during stage 1. Calculations of solution chemistry via Visual MINTEQ showed that the pH drop was due to the formation of ion pairs between calcium ions and phosphate species, which increased the ratio of free acidic phosphate species (supplementary information, section C and Table S2) [16]. When the titration of calcium solution was complete, solution pH showed a stable value during stage 2, corresponding to the metastable supersaturated solution. The first discernible drop in pH remarked the appearance of the first new phase in the solution and the start of stage 3. Observations of the pH change was accompanied by visual changes in solution turbidity shortly after, verifying precipitation. Characterization of the solid phase at stage 3 by FTIR showed broad  $\text{PO}_4^{3-}$  bands near  $1040\text{ cm}^{-1}$ , and a weak band at  $875\text{ cm}^{-1}$  associated with  $\text{HPO}_4^{2-}$ . XRD analysis showed no diffraction peaks, which together with FTIR data indicated presence of an amorphous calcium phosphate phase (ACP) (Figure 2). The drop in pH at stage 3 was followed by a short plateau, which can be interpreted as the solution reaching a steady state, in equilibrium with the ACP. Accordingly, the second drop of pH was interpreted as the emergence of a second phase in the system and determined the onset of stage 4. Characterization of precipitates by XRD showed diffraction peaks associated with poorly crystalline apatite and the distinguishing peak for octacalcium phosphate (OCP) was observed at  $2\theta$   $4.7^\circ$  (Figure 2b). FTIR data supported the crystal formation via sharp  $\text{PO}_4^{3-}$  peaks at  $1025$  and  $962\text{ cm}^{-1}$  and splitting of the  $\nu_4$  bending of  $\text{PO}_4^{3-}$  at  $600$  and  $560\text{ cm}^{-1}$ , indicating apatite crystallization [17]. SEM images of samples collected at stage 3 and stage 4 showed aggregated spherical ACP particles and flake-like apatite precipitates, respectively (Figure 3).

The two-step precipitation pathway observed here is common when the initial solution is supersaturated with respect to ACP, due to its fast precipitation kinetics.

Since the solution was still supersaturated with respect to crystalline phases of calcium phosphate after ACP precipitation at stage 3, nucleation of a new phase was probable and initiated the phase transformation in the system towards the more stable product. In the presence of macromolecular additives, both the precipitation pathway and the kinetics of each precipitation step can be affected, which could give insights on the interaction modes between the organic and inorganic components [18, 19]. Correspondingly, the effects of fetuin-A on mineralization of CaP were investigated.

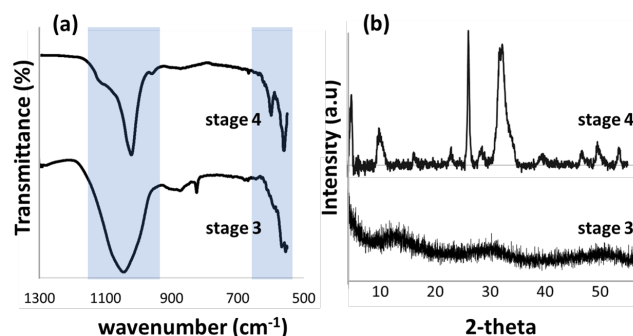


**Figure 2.** (a) FTIR and (b) XRD spectra of precipitates collected at stage 3 (bottom) and stage 4 at the end of experiments (top). The areas shaded in blue in FTIR spectra highlight the changes in the peak widths and positions.

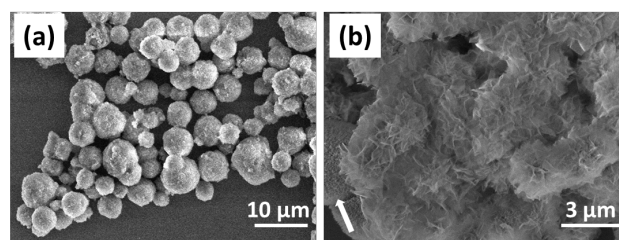


**Figure 3.** SEM images of the particles collected at (a) stage 3 and (b) stage 4. The arrow in (b) shows a remaining spherical particle showing incomplete phase transformation.

### 3.1.1. Effect of Fetuin-A on mineral formation

The precipitation experiments were repeated in the presence of varying concentrations of fetuin-A. The pH curves showed the same characteristic 2-step behavior with plateaus observed at comparable values for all experimental conditions and similar pH change during titration of calcium solution during stage 1, but with drastic changes in the duration of subsequent stages (Figure 4). The pH data revealed that the presence of fetuin-A did not induce a change in the precipitation pathway, which was secondarily supported by the SEM images of precipitates collected during the subsequent stages of the reaction in the presence of the highest fetuin-A concentration (supplementary the information, section D). It was shown that succeeding stages of the reaction were associated with typical morphologies of

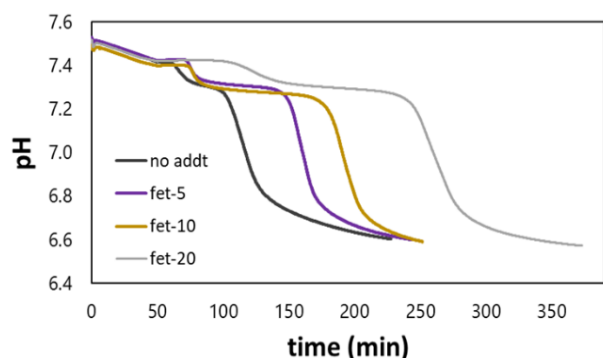


**Figure 4.** pH curves without additive and with varying concentrations of fetuin-A as a function of time.

amorphous spheres at stage 3 and formation of crystalline flakes at stage 4. However, fetuin-A greatly affected the kinetics of the precipitation reactions. The lifetime of the metastable solution prior to precipitation (duration of stage 2) and lifetime of ACP phase (duration of stage 3) were investigated as a function of fetuin-A concentration (Figure 5). Data showed significant prolongation in stage 2, with a parabolic dependence on protein concentration. The delay in the formation of ACP in the presence of molecular additives could be related to (i) an effective drop in the calcium activity due to protein binding, thus lowering of supersaturation, and/or (ii) interruption of fetuin-A with kinetics of mineral formation [20, 21]. Supersaturation, constituting the thermodynamic driving force for precipitation, affects both the nucleation and growth rates of solids. In-situ measurements of calcium activity during the titration of calcium solution (stage 1) showed that in the presence of fetuin-A, the calcium activity was lowered in a concentration dependent manner, reaching a 12% reduction at the highest concentration of the additive (fet-20) (Figure 6). In the absence of protein, the calcium activity measurements matched very closely with the thermodynamically calculated values shown by blue dots on Figure 5, which takes into account the amount of calcium added to the system and the ion association complexes it would form with phosphate species. However, when fetuin-A is present in the reaction medium, calcium activity was measured at lower values indicating binding of calcium by the protein via its high affinity aspartic and glutamic acid rich residues [8]. Thermodynamic calculations with the lowest calcium activity measured at fet-20 conditions showed that initial solution supersaturation was lowered to  $S_{HA} = 23.9$ . When the kinetic factors of nucleation are considered, presence of fetuin-A can decrease the nucleation rate by interfering with the incoming flux of monomers to the nuclei surface or block the nucleation sites, as commonly observed in precipitation systems in the presence of additives [22]. Thus, it was concluded that the presence of fetuin-A could inhibit ACP formation via both thermodynamic and kinetic effects.

The lifetime of ACP, specified by the duration of stage 3, was also prolonged and showed a linear dependence to the fetuin-A concentration. Earlier work suggested that such a dependence on additive concentration signals to adsorption of additives on the surface of the metastable phase [17, 23]. They can then hinder the phase transition either via inhibition of heterogeneous nucleation of the new phase on the metastable precursor, or via slowing down the dissolution process of the metastable phase, which consequently hinders the availability of constituent ions for the new phase formation.

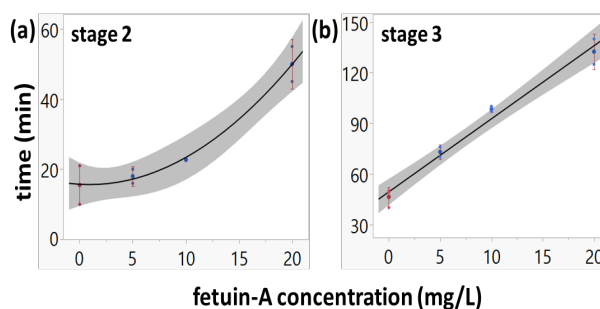


**Figure 5.** The duration of (a) stage 2 and (b) stage 3 as a function of fetuin-A concentration. The grey shaded area marks the 95% confidence interval.

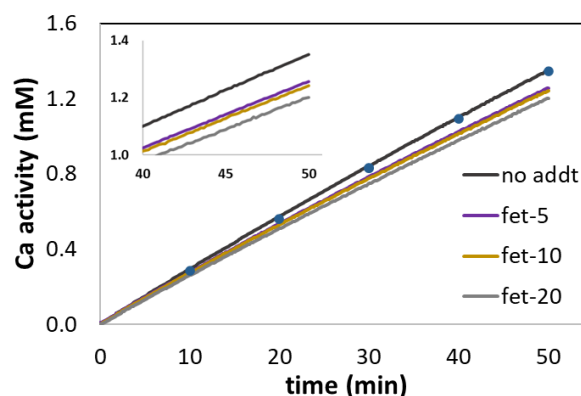


**Figure 6.** In situ measurements of calcium ion activity during the titration of calcium solution without and with varying concentration of fetuin-A. Blue dots denote the theoretically calculated values of activity, showing a close match with additive-free experiments.

Yet, we cannot differentiate between the active inhibition mechanism of the fetuin-A within the scope of this work. In order to make such deductions, quantitative analysis of adsorbed protein as a function of initial additive concentration would be required in combination with high resolution *in situ* or cryogenic methods such as TEM, to follow the mode of nucleation for the emerging phase.

The characterization of final precipitates with XRD showed that in the presence of lower concentrations of fetuin-A, the final precipitates were not altered (Figure 7). However, with the fetuin-A concentration of 20 mg in the reaction medium, the final precipitate was composed of HA only, as shown by the absence of OCP peak in the XRD spectrum. The change in composition could be induced by the prolonged reaction time, where the thermodynamically more stable HA dominates the final composition. OCP could still have precipitated in the system and phase transformed to HA completely during the course of the reaction. Yet, without further time-resolved analysis, this hypothesis cannot be confirmed. SEM images of final precipitates showed structural changes with the flake-like structures being composed of thicker plates at highest fetuin-A concentration (Figure 8).

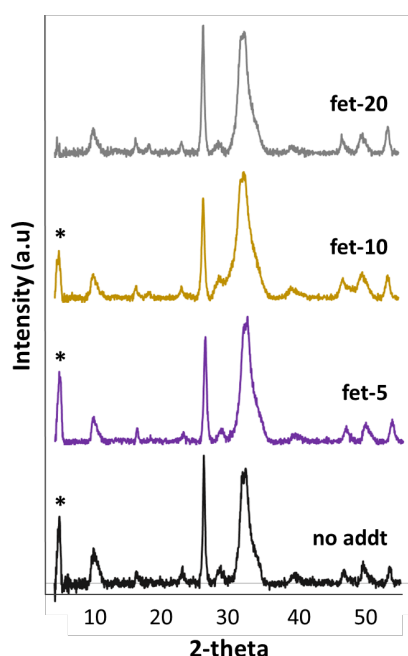


**Figure 7.** XRD spectra of final precipitates with asterisk marking the distinguishing OCP peak.

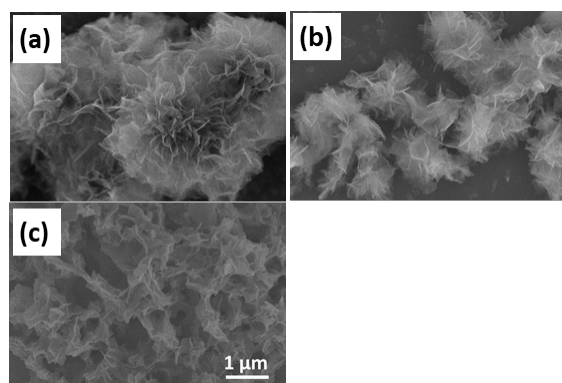


**Figure 8.** SEM images of precipitates collected at the end of experiments with fetuin-A additive in concentrations of (a) 5, (b) 10 and (c) 20 mg.

#### 4. Conclusion

The role of fetuin-A in inhibition of mineral formation was investigated in a two-step precipitation pathway. It was shown that the presence of fetuin-A lowers the calcium ion activity through binding of ions and prolong the precipitation time for ACP. Yet, after its formation ACP was stabilized by the protein against phase transformation, most likely via surface adsorption. We anticipate the findings in this study will improve the understanding of mineralization inhibition mechanisms by the additives, and, in turn contribute to the design of enhanced treatment methods towards ectopic mineralization.

#### Acknowledgement

The Research Council of Norway is acknowledged for the support to the Norwegian Center for Transmission Electron Microscopy, NORTEM (197405/F50), and the Norwegian Micro- and Nano-Fabrication Facility, NorFab (295864).

#### Author's Contributions

**Şeniz Uçar:** Conceptualized the study, performed the experiments and analyses of result, drafted and wrote the manuscript.

#### Ethics

There are no ethical issues after the publication of this manuscript.

#### References

- [1]. Mann, S., 1988, Molecular recognition in biomineralization. *Nature*, 332(6160): p. 119-124.
- [2]. Meldrum, F.C. and H. Cölfen, 2008, Controlling Mineral Morphologies and Structures in Biological and Synthetic Systems. *Chemical Reviews*, 108(11): p. 4332-4432.
- [3]. Eidelman, N., L.C. Chow, and W.E. Brown, 1987, Calcium phosphate saturation levels in ultrafiltered serum. *Calcified Tissue International*, 40(2): p. 71-78.
- [4]. Cai, M.M., E.R. Smith, and S.G. Holt, 2015, The role of fetuin-A in mineral trafficking and deposition. *Bonekey Rep*, 4: p. 672.
- [5]. Xu, A.-W., Y. Ma, and H. Cölfen, 2007, Biomimetic mineralization. *Journal of Materials Chemistry*, 17(5): p. 415-449.
- [6]. Gelli, R., F. Ridi, and P. Baglioni, 2019, The importance of being amorphous: calcium and magnesium phosphates in the human body. *Advances in Colloid and Interface Science*, 269: p. 219-235.
- [7]. Trepanowski, J.F., J. Mey, and K.A. Varady, 2015, Fetuin-A: a novel link between obesity and related complications. *International Journal of Obesity*, 39(5): p. 734-741.
- [8]. Heiss, A., et al., 2003, Structural basis of calcification inhibition by  $\alpha$ -2-HS glycoprotein/fetuin-A: Formation of colloidal calciprotein particles. *Journal of Biological Chemistry*, 278(15): p. 13333-13341.

- [9]. Brylka, L. and W. Jahnhen-Dechent, 2013, The Role of Fetuin-A in Physiological and Pathological Mineralization. *Calcified Tissue International*, 93(4): p. 355-364.
- [10]. Schinke, T., et al., 1996, The serum protein  $\alpha$ 2-HS glycoprotein/fetuin inhibits apatite formation in vitro and in mineralizing calvaria cells. A possible role in mineralization and calcium homeostasis. *Journal of Biological Chemistry*, 271(34): p. 20789-20796.
- [11]. Seto, J., et al., 2012, Accelerated Growth Plate Mineralization and Foreshortened Proximal Limb Bones in Fetuin-A Knockout Mice. *PLoS ONE*, 7(10).
- [12]. Price, P.A. and J.E. Lim, 2003, The inhibition of calcium phosphate precipitation by fetuin is accompanied by the formation of a fetuin-mineral complex. *Journal of Biological Chemistry*, 278(24): p. 22144-22152.
- [13]. Rochette, C.N., et al., 2009, A shielding topology stabilizes the early stage protein-mineral complexes of fetuin-A and calcium phosphate: A time-resolved small-angle x-ray study. *ChemBioChem*, 10(4): p. 735-740.
- [14]. Pasch, A., et al., 2012, Nanoparticle-Based Test Measures Overall Propensity for Calcification in Serum. *Journal of the American Society of Nephrology*, 23(10): p. 1744-1752.
- [15]. Heiss, A., et al., 2007, Structural dynamics of a colloidal protein-mineral complex bestowing on calcium phosphate a high solubility in biological fluids. *Biointerphases*, 2(1): p. 16-20.
- [16]. Ucar, S., et al., 2019, Formation of Hydroxyapatite via Transformation of Amorphous Calcium Phosphate in the Presence of Alginate Additives. *Crystal Growth and Design*, 19(12): p. 7077-7087.
- [17]. Chen, Y., et al., 2014, Stabilizing amorphous calcium phosphate phase by citrate adsorption. *CrystEngComm*, 16(10): p. 1864-1867.
- [18]. Fang, W., et al., 2016, Hydroxyapatite Crystal Formation in the Presence of Polysaccharide. *Crystal Growth & Design*, 16(3): p. 1247-1255.
- [19]. Hu, Q., et al., 2012, The thermodynamics of calcite nucleation at organic interfaces: Classical vs. non-classical pathways. *Faraday Discussions*, 159: p. 509-523.
- [20]. Zou, Z., et al., 2018, Additives influence the phase behavior of calcium carbonate solution by a cooperative ion-association process. *Journal of Materials Chemistry B*, 6(3): p. 449-457.
- [21]. Ibsen, C.J.S., D. Gebauer, and H. Birkedal, 2016, Osteopontin Stabilizes Metastable States Prior to Nucleation during Apatite Formation. *Chemistry of Materials*, 28(23): p. 8550-8555.
- [22]. Westin, K.J. and Å.C. Rasmuson, 2005, Nucleation of calcium carbonate in presence of citric acid, DTPA, EDTA and pyromellitic acid. *Journal of Colloid and Interface Science*, 282(2): p. 370-379.
- [23]. Ding, H., et al., 2014, Toward a Detailed Understanding of Magnesium Ions on Hydroxyapatite Crystallization Inhibition. *Crystal Growth & Design*, 14(2): p. 763-769.